

Spin and interaction effects in Shubnikov–de Haas oscillations and the quantum Hall effect in GaN/AlGaN heterostructures

This article has been downloaded from IOPscience. Please scroll down to see the full text article.

2004 J. Phys.: Condens. Matter 16 3421

(<http://iopscience.iop.org/0953-8984/16/20/013>)

View [the table of contents for this issue](#), or go to the [journal homepage](#) for more

Download details:

IP Address: 129.252.86.83

The article was downloaded on 27/05/2010 at 14:39

Please note that [terms and conditions apply](#).

Spin and interaction effects in Shubnikov–de Haas oscillations and the quantum Hall effect in GaN/AlGaN heterostructures

W Knap^{1,2}, V I Fal'ko³, E Frayssinet⁴, P Lorenzini⁴, N Grandjean⁴,
D Maude⁵, G Karczewski^{6,9}, B L Brandt⁶, J Łusakowski^{5,10}, I Grzegory²,
M Leszczyński², P Prystawko², C Skierbiszewski², S Porowski², X Hu⁷,
G Simin⁷, M Asif Khan⁷ and M S Shur⁸

¹ GES, UMR5650 CNRS—Université Montpellier2, 34095 Montpellier, France

² High Pressure Research Centre, PAN-UNIPRESS, 01142 Warsaw, Poland

³ Physics Department, Lancaster University, LA1 4YB, UK

⁴ CNRS-CRHEA, rue Bernard Grégory, F-06560 Valbonne-Sophia-Antipolis, France

⁵ Grenoble High Magnetic Field Laboratory, CNRS-MPI, 38000 Grenoble, France

⁶ National High Magnetic Field Laboratory, Florida State University, Tallahassee, FL 32310, USA

⁷ Department of ECE, University of South Carolina, Columbia, SC 29208, USA

⁸ Department of ECSE and Broadband Center, Rensselaer Polytechnic Institute, Troy, NY 12180, USA

E-mail: knap@ges.univ-montp2.fr

Received 9 January 2004

Published 7 May 2004

Online at stacks.iop.org/JPhysCM/16/3421

DOI: 10.1088/0953-8984/16/20/013

Abstract

We present the results of high magnetic field (up to 30 T) and temperature (50 mK–80 K) dependent transport measurements on a 2DEG in GaN/AlGaN heterojunctions. A high mobility (above 60 000 cm² V⁻¹ s⁻¹ at 4 K) 2DEG was obtained by MBE growth of dislocation free GaN and AlGaN layers on semi-insulating bulk GaN substrates. A cyclotron gap and spin splitting are observed. Results from two studies are reported: (i) a tilted field experiment determining the 2DEG g^* -factor from the angular modulation of the amplitude of SdH oscillations; (ii) quantum Hall effect measurements determining the activation energies for spin and cyclotron energy gaps at even and odd filling factors. The observed ‘cyclotron gap’ enhancement is attributed to the effect of electron–electron interaction and it is estimated using the model of a 2D-screened Coulomb potential. The analytic result for the enhancement of the ‘cyclotron gap’ yields an addition to the activation energy, $\mathcal{E}_{\text{even}}^x \approx \kappa \hbar \omega_c$, $\kappa = 1.06\sqrt{a^2 n_e}$, which is proportional to the magnetic field and resembles the mass renormalization.

⁹ On leave from: Institute of Physics, Polish Academy of Sciences, Warsaw, Poland.

¹⁰ On leave from: Institute of Experimental Physics, Warsaw University, Warsaw, Poland.

1. Introduction

GaN and its alloys with Al and In have attracted much attention fuelled by their potential for applications in high power electronics and electro-optic devices [1, 2]. Since the demonstration of the existence of a two-dimensional electron gas (2DEG) at the AlGaIn/GaN interface [3, 4] substantial progress has been achieved in improving electron mobility in AlGaIn/GaN heterojunctions deposited on various substrates [5–7]. High quality of these structures has enabled study of the cyclotron resonance in these systems [4], and also observation of both even and odd integer quantum Hall effects (QHE) [4, 5, 8]. Note that 2DEGs in GaN can be seen as a particularly convenient system for studying spin-polarization and electron–electron correlation effects due to the heavy mass of electrons (according to [4]¹¹, $m^* = 0.23\text{--}0.25 m_e$, where m_e is the free electron mass) and a g -factor close to the free electron value [9]. In particular, even at relatively high electron concentrations $n_e \sim 10^{12} \text{ cm}^{-2}$, a large value of the r_s parameter can be achieved, where $r_s^{-1} = \sqrt{a^2 n_e}$, $a = \chi \hbar^2 / e^2 m^*$ is the donor related Bohr radius and $\chi = 8.9$ is the dielectric constant.

Also due to the heavy mass of electrons and a g -factor close to the free electron value the ratio of the Zeeman energy (E_Z) to the cyclotron energy ($\hbar\omega_c$) is more than one order of magnitude higher than in the traditionally studied GaAs based 2DEG. This means in particular that the condition of equality of the cyclotron and Zeeman energies $E_Z = (n + \frac{1}{2})\hbar\omega_c$ (where $E_Z = \mu g^* B$, μ is the Bohr magneton and $\omega_c = eB \cos\theta / m^* c$ is the frequency cyclotron motion of 2D electrons) can be obtained for relatively small tilt angles θ (this is the angle between the magnetic field and the direction of growth of the heterojunction). Therefore the 2DEG in a GaN system is an appealing object for studies of modulation of the amplitude of Shubnikov–de Haas oscillations (SdHO) induced by spin splitting and varied by the magnetic field tilting [9, 10].

The main problems in experimental studies of the 2DEG in GaN are related to: (i) relatively low electron mobility and (ii) the presence of substrate related parasitic conducting channels [6, 11]. The limitations of the low temperature mobility in GaN/AlGaIn heterostructures are mainly due to the presence of dislocations. The dislocations which usually spoil the mobility of heterojunctions made on sapphire and SiC substrates can be eliminated by using high pressure grown crystalline bulk substrates [5]. High pressure bulk substrates can also be made semi-insulating by magnesium doping. Therefore 2DEG structures made on them allow making transport activation measurements without any parasitic/parallel conduction channels. In this paper, we present the results of magnetotransport studies of high mobility samples which were obtained by homoepitaxy deposition of GaN and AlGaIn layers on magnesium doped semi-insulating bulk substrates. The mobility of the structures used in this work exceeded $60 \times 10^3 \text{ cm}^2 \text{ V}^{-1} \text{ s}^{-1}$, and there was no parallel conduction over the whole temperature range investigated.

In section 2, we report the results of transport measurements performed on high mobility GaN/AlGaIn structures both in the regimes of large and small filling factors ν and at low and high temperatures. For large filling factors ν between 20 and 40 (the semiclassical SdHO regime), we studied the dependence of the SdHO on the tilt angle θ . We observed that the

¹¹ The effective mass of the 2DEG in different GaN/AlGaIn heterojunctions was earlier measured in cyclotron resonance experiments [4]. It was shown that it depends on the carrier density due to important nonparabolicity corrections. Also the polaron corrections have to be taken into account. The cyclotron resonance determined effective mass was found to be $m^* = 0.24$ and $0.25 m_e$ for the carrier densities 4×10^{12} and $9 \times 10^{12} \text{ cm}^{-2}$, respectively. The value of the effective mass can be found from an empirical formula based on the two-band nonparabolicity approximation: $m^*/m_e = 0.230 + 2(E^0/3 + E_F)/E_g$ where E^0 is the energy of the first electrical level, E_F is the Fermi energy and E_g is the GaN energy gap. For the carrier density $2.4 \times 10^{12} \text{ cm}^{-2}$ studied in this work, the calculated effective mass was $m^* = 0.238 \pm 0.02 m_e$.

diagonal element of the conductivity tensor, σ_{xx} , oscillates with the magnetic field and tilt angle according to the law

$$\frac{\sigma_{xx}(\nu, \theta)}{\sigma_0} = 1 - \frac{Ae^{-\pi/\tau_q\omega_c}}{\sinh A} \cos\left(\frac{\pi g^* m^*}{2m_e \cos\theta}\right) \cos(\pi\nu), \quad (1)$$

where $A = 2\pi^2 kT/\hbar\omega_c$, σ_0 is the conductivity at zero magnetic field and τ_q is the quantum scattering time. The formula reveals a modulation in the SdHO amplitude accompanied by a π -shift in the phase of oscillations. The latter happens under the condition $(n + \frac{1}{2})\hbar\omega_c(B \cos\theta) = E_Z$ driven by the magnetic field tilting with respect to the normal to the 2DEG plane.

In section 3, we analyse the transformation of SdHO into pronounced quantum Hall effect minima in σ_{xx} and determine the activation energy gaps, \mathcal{E}_ν , for small integer filling factors, $10 > \nu > 4$:

$$\sigma_{xx} \propto \exp(-\mathcal{E}_\nu/2kT). \quad (2)$$

We compare the magnetic field dependence of the ‘spin’ (\mathcal{E}_{2n+1}) and ‘cyclotron’ (\mathcal{E}_{2n+2}) gaps obtained with the single-particle Landau level splittings. For odd filling factors we were not able to distinguish between the observed values of the ‘spin’ gap \mathcal{E}_{2n+1} and the single-particle Zeeman splitting energy with the g -factor obtained from the low field beats analysis, $\mathcal{E}_{2n+1} \approx E_Z = g^* \mu_B$. For even filling factors ($\nu = 4, 6, 8, 10$) we found that the activation energy increases faster in a rising magnetic field, as compared to the single-particle inter-Landau level splitting, $\mathcal{E}_{2n+2} = \hbar\omega_c - E_Z + \kappa\hbar\omega_c - \Gamma$. The observed value of the effective activation energy enhancement is interpreted in terms of the dissociation energy of the inter-Landau level magneto-exciton enhanced by the exchange interaction [12–15]. The calculation using the model with a screened electron–electron repulsion potential in a 2D gas is described in section 3. The analytic result for the enhancement of the ‘cyclotron gap’ yields an addition to the activation energy which is proportional to the cyclotron energy, $\kappa\hbar\omega_c$, and which resembles the ‘cyclotron’ gap renormalization with $\kappa = 1.06/r_s$ and represents the first term in the expansion in the inverse of r_s for large r_s .

2. Modulation of the SdH oscillation amplitude due to magnetic field tilting

Dislocation free high quality AlGaIn/GaN heterostructures studied in the present work have been grown using NH_3 molecular beam epitaxy on the Ga face of semi-insulating bulk GaN substrates [16]. The sample had a mesa-etched Hall bar geometry, $600 \mu\text{m}$ (length) \times $100 \mu\text{m}$ (width). Ohmic contacts were obtained by Ni–In evaporation followed by rapid thermal annealing. Hall measurements were performed on these samples from 80 K down to 50 mK.

Two runs of magnetotransport measurements were performed. First, the tilted field experiment was carried out in Grenoble HMFL using a superconducting coil ($B < 15$ T) coupled with a dilution refrigerator. It used a sample holder that allowed us to rotate the sample with respect to the magnetic field direction inside the dilution refrigerator (He bath temperature $T = 50$ mK). In these measurements, a low frequency (10 Hz) alternating current method was used, with $I < 100$ nA, and Hall and longitudinal voltages were registered simultaneously in two independent lock-in channels. The surface carrier density, as determined from the period of the SdHO, was $n_e = 2.4 \times 10^{12} \text{ cm}^{-2}$. Typical results for $R_{xx}(B)$ and $R_{xy}(B)$ are shown in figure 1, which exhibits a pronounced quantum Hall effect (QHE) behaviour at $\nu = 7$ –9. From the analysis of the SdHO (see the inset to figure 1) and the low temperature mobility, the quantum scattering time, τ_q , and the transport scattering time, τ_p , were found to be 0.4 and 8.2 ps, respectively [5]. It is important to note that even in these high mobility samples the disorder was high enough to produce a quantum time $\tau_q \sim 0.4$ ps that corresponds to a substantial Landau level broadening. The large value of the ratio $\tau_p/\tau_q \sim 20$ indicates the

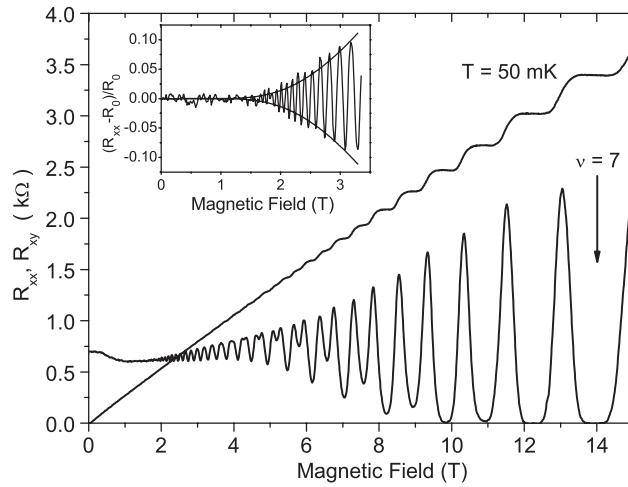


Figure 1. Longitudinal R_{xx} and transverse R_{xy} magnetoresistance versus magnetic field at 50 mK. The inset shows the low field part of the SdHO after normalization by the low field resistance value, R_0 , and the fit of the SdHO amplitude. The arrow marks the magnetic field corresponding to $\nu = 7$.

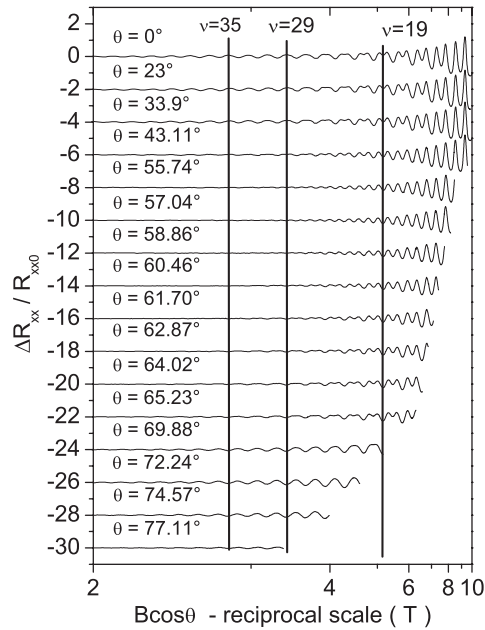


Figure 2. Longitudinal magnetoresistance R_{xx} for different tilt angles. The resistance is normalized by its value at zero magnetic field R_{xx0} . Different traces are shifted in the y direction for clarity. The x axis is the magnetic field perpendicular to the 2D gas plane. A reciprocal scale, in which the SdHO are periodic, is used. The vertical lines mark a few characteristic filling factors $\nu = 35, 29, 19$. They are ‘guides for the eye’ showing the change of the phase of the SdH oscillations.

long range character of a disordered potential, or may be attributed to a weak inhomogeneity of the 2D electron density.

Figure 2 shows traces for the SdHO studied in the same sample at various tilt angles. They are plotted as a function of a perpendicular magnetic field component, $B \cos \theta$, using a

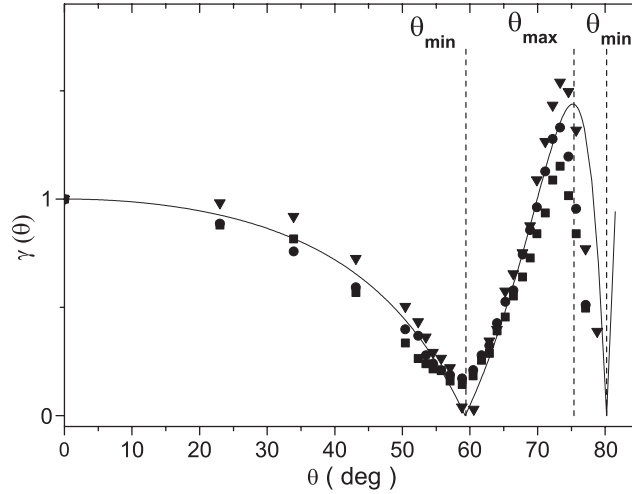


Figure 3. Normalized Shubnikov–de Haas amplitude for filling factors $\nu = 30$ (circles), $\nu = 32$ (squares) and $\nu = 35$ (triangles), as a function of the tilt angle. The continuous curve is the fit using equation (4).

reciprocal scale. They manifest that the amplitude and phase of oscillations change with the tilt angle, θ . For instance, maxima observed for filling factors $\nu = 35$ and 29 for $\theta = 0^\circ$ transform into minima for $\theta = 74.6^\circ$, with the amplitude dropping down to almost zero at $\theta = 60^\circ$, which is accompanied by a noticeable frequency doubling between filling factors 29 and 19 around $\theta \approx 60^\circ$.

The reduction in the amplitude of the SdHO upon tilting is related to a condition $E_Z = (n + \frac{1}{2})\hbar\omega_c$ and two series of spin up (+) and spin down (−) Landau levels, $\varepsilon_{n\pm} = (n + \frac{1}{2})\hbar\omega_c \pm \frac{1}{2}E_Z$, becoming equidistant from each other, as illustrated in figure 4. In a semiclassical limit, this effect can be described as an overlap of two oscillatory contributions σ_+ and σ_- to the 2D conductivity coming from two parallel conduction channels related to spin-polarized 2D electrons with a common Fermi level, E_F :

$$\frac{\sigma_{\pm}}{\sigma_0} = \frac{1}{2} - \frac{A}{2 \sinh A} e^{-\pi/\tau_q\omega_c} \cos\left(2\pi \frac{E_F \mp E_Z/2}{\hbar\omega_c}\right). \quad (3)$$

Therefore, the oscillating part in the total conductivity of the 2D gas is the sum of two oscillating dependences in equation (3):

$$\sigma_{xx} = \sum_{\pm} \sigma_{\pm} = \sigma_0 - \sigma_{osc}(\theta) \cos(\pi\nu)$$

shifted in phase by $2\pi E_Z/\hbar\omega_c$, which yields the result quoted in equation (1).

The first minimum in the SdHO amplitude described in equation (1) occurs for the tilt angle $\cos\theta = g^*m^*/m_e$; this is followed by a rise of the amplitude of oscillations up to a value higher than that expected in a perpendicular magnetic field. The position of such a minimum can be used to determine the 2D electron g -factor, as shown in figure 3. The experimental data (dots) in figure 3 are compared to the theoretical expectation (solid curve) for the amplitude of the SdHO [9] normalized by its value in a perpendicular field:

$$\gamma(\theta) = \frac{\sigma_{osc}(\theta)}{\sigma_{osc}(0)} = \frac{\cos\left(\frac{\pi g^* m^*}{2m_e \cos\theta}\right)}{\cos\left(\frac{\pi g^* m^*}{2m_e}\right)}, \quad (4)$$

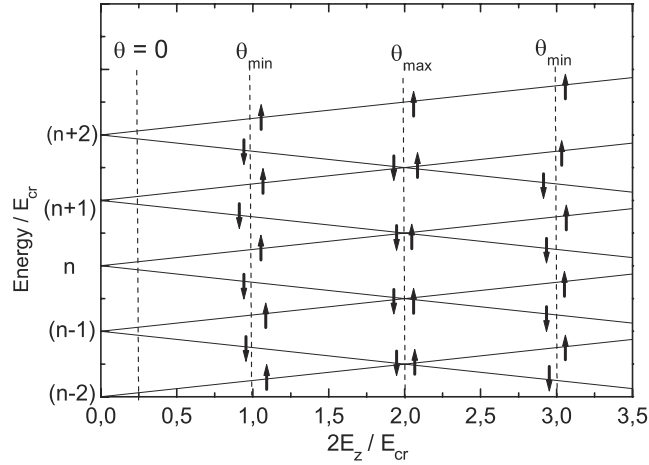


Figure 4. A schematic representation of a few consecutive Landau levels as a function of the Zeeman splitting. Dotted vertical lines indicate characteristic angles for which the minima (ν_{\min}) and maxima (ν_{\max}) of the SdHO amplitude are expected.

which represents the best single-parameter fit of the result in equation (4) and corresponds to $g^* \approx 2.14 \pm 0.06$. The effective mass was taken $m^* = 0.238 \pm 0.02 m_e$ (see footnote 11). The SdHO show a pronounced minimum in the oscillation amplitude at about $\theta_{\min} \approx 60^\circ$, which is accompanied by their π -shift seen in the raw data; figure 3. The minimum is followed by the maximum at $\theta_{\max} \approx 73^\circ$, the angle providing the crossing of two neighbouring spin-split Landau levels and, therefore, a maximal single-particle energy splitting exactly equal to the cyclotron energy. For larger angles, the system approaches the condition $\frac{3}{2}\hbar\omega_c = E_Z$ for which the next minimum, $\theta_{\min} \approx 80^\circ$, in the SdHO amplitude occurs. One can notice that the true disappearance of oscillations associated with the π -shift in their phase takes place only at larger filling factors, $\nu > 32$. For smaller filling factors, the transformation of the conductivity minimum into a maximum upon increasing the tilt angle passes the stage (a narrow interval in θ) where the frequency of oscillations is doubled. This is the manifestation of the formation of a real gap in the spectrum of conducting electron states, that is, a precursor of the quantum Hall effect which is more pronounced at smaller filling factors, $\nu < 8$. The evolution of the SdHO with tilt angle was partially observed and interpreted for lower quality samples of GaN 2DEG on sapphire [9]. Lower electron mobility and the presence of the parallel conduction allowed us to observe clearly only the first minimum ($\frac{1}{2}\hbar\omega_c = E_Z$) in the amplitude versus angle dependence (see figure 3). The high quality of the samples on the bulk GaN used in this work allowed us to follow the SdHO through the crossing of the adjacent Landau levels ($\hbar\omega_c = E_Z$; see figure 4) and up to the $\frac{3}{2}\hbar\omega_c = E_Z$ condition. The results presented here are also in a very good agreement with recent theoretical works [17] and confirm that 2DEG in GaN can be considered as a very convenient system for studying the influence of the spin splitting on the modulation of Shubnikov–de Haas oscillations.

3. Quantum Hall effect and energy gap enhancement at even integer filling factors

The second experiment was performed using a perpendicular magnetic field up to 30 T from a resistive Bitter magnet in Tallahassee-NHMFL and in the temperature range $2 \text{ K} < T < 80 \text{ K}$. The sample was placed in a stainless steel closed sample holder with a few mbar pressure of

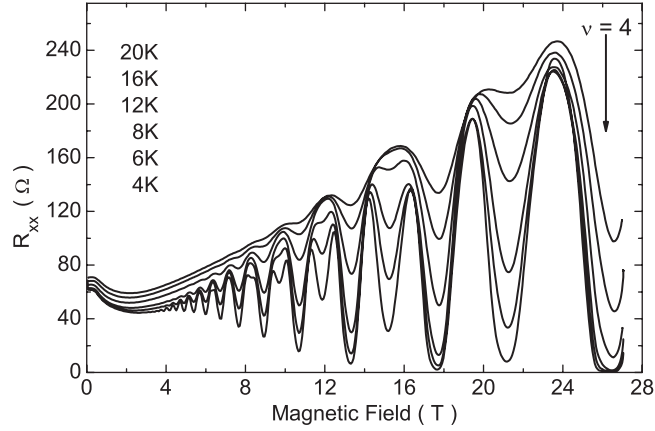


Figure 5. The longitudinal magnetoresistance R_{xx} for temperatures of 4 (lowest trace), 6, 8, 12, 16, 20 K (highest trace). The arrow marks the magnetic field corresponding to $\nu = 4$.

helium gas. The sample holder was directly immersed in the liquid helium bath, for better heat exchange. The temperature was regulated using a resistive heater and special care was taken with temperature measurements and stabilization. In order to avoid the influence of the high magnetic field a capacitive temperature sensor was used in the temperature controller feedback loop. The direct current method was used, with currents varying between 1 and 10 μA . The 2D carrier density in the heterostructure varied slightly between cooling cycles, as $n_e^\blacksquare = 2.4 \times 10^{12} \text{ cm}^{-2}$ and $n_e^\blacktriangle = 2.6 \times 10^{12} \text{ cm}^{-2}$.

In figure 5 we show the measured temperature dependence of the SdHO in R_{xx} and the formation of quantum Hall effect minima at filling factors 4–8. We use the Arrhenius plot for the temperature dependence of R_{xx} in the minima at odd and even integer filling factors to obtain the values of the activation energy. The Arrhenius plots for the minima of R_{xx} at even filling factors $\nu = 4, 6, 8$ and 10 in samples with almost identical densities, $n_e^\blacksquare = 2.4 \times 10^{12} \text{ cm}^{-2}$ and $n_e^\blacktriangle = 2.6 \times 10^{12} \text{ cm}^{-2}$, are shown in the inset to figure 6.

The activation energies determined from these plots and shown in figure 6 are related to the inter-Landau level excitations. They cannot be easily related to the single-particle energy splitting, $\hbar\omega_c - E_Z - \Gamma$, between percolating states identified with the centres of broadened Landau levels $(n, +)$ and $(n+1, -)$, at both low and high magnetic fields. Following the method proposed in [18] (that shows how to analyse the magnetic field dependence of the activation energy data), we approximate the data for \mathcal{E}_{2n+2} using a linear fit, $\mathcal{E}(B) = \hbar\omega_c - E_Z - \Gamma + \kappa\hbar\omega_c$, where the electron mass and g -factor are those quoted above, and two fitting parameters, Γ and κ , are equal to $\Gamma = 47.4 \pm 3.2 \text{ K}$ and $\kappa \approx 0.43 \pm 0.02$. Following [18], we attribute the offset value Γ to the inelastic Landau level broadening that gives the percolation state a finite width, and $\kappa\hbar\omega_c$ to a possibility that the inter-Landau level excitation energy can be enhanced by the interaction effects. Since at $\nu = 4, 6, 8, 10$ the excitation energy of a carrier activated from the chemical potential level into the percolating state is quite large, electron relaxation from a percolating state towards lower energy localized states may go fast. This makes a great difference, as compared to the odd integer filling factor case, where the relaxation both involves a smaller energy transfer and requires a spin-flip process (the latter is particularly improbable in GaN).

On the other hand, in the regime of high magnetic fields providing a large enough splitting between occupied and empty Landau levels, $\hbar\omega_c - E_Z > \Gamma, \hbar/\tau_q$, the activation energy of

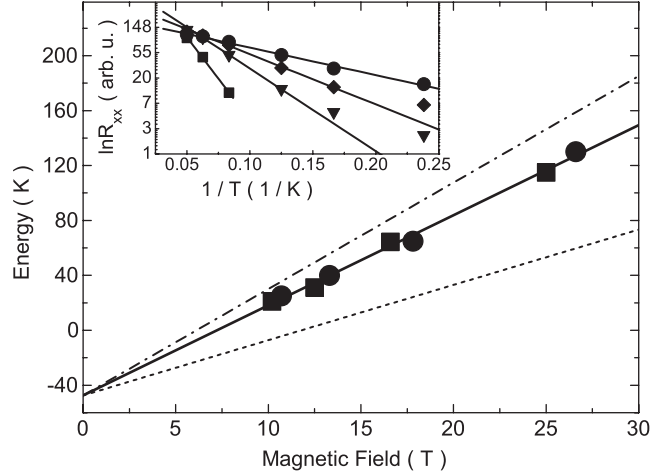


Figure 6. Activation energies for even filling factors $\nu = 4, 6, 8, 10$ as a function of magnetic field. Circles and squares represent results for two different carrier densities 2.4 and $2.6 \times 10^{12} \text{ cm}^{-2}$ respectively. The continuous line is the linear fit to the data (shift $-47.4 \pm 3.2 \text{ K}$, linear coefficient $6.6 \pm 0.2 \text{ K T}^{-1}$). The dashed line (coefficient 4 K T^{-1}) corresponds to the cyclotron energy minus the spin energy and was shifted down by the Landau level width. The dotted–dashed line (coefficient 7 K T^{-1}) corresponds to theoretical calculations. The inset shows Arrhenius plots of R_{xx} data with linear fits: for filling factors $\nu = 4$ (lowest line), 6, 8 and 10 (highest line).

a pair consisting of an electron at the ‘upper’ filled Landau level ($n + 1, -$) and a ‘hole’ at the ‘lower’ empty Landau level ($n, +$) is enhanced by a contribution equal to the dissociation energy \mathcal{E}_{2n+2}^x of the inter-Landau level magneto-exciton [13, 19, 12]. For the filling factor $\nu = 2n + 2$, the latter can be represented in the form

$$\mathcal{E}_{2n+2}^x = (n + 1) \int_0^\infty \frac{e^{-x}}{x} [L_n(x) - L_{n+1}(x)]^2 V(\lambda\sqrt{2x}) dx, \quad (5)$$

where L_n is the Laguerre polynomial, $V(r)$ is the effective electron–electron repulsion interaction and $\lambda = \sqrt{\hbar c/eB}$ is the magnetic length. For the unscreened Coulomb interaction usually discussed in application to the activation energy problem in incompressible QHE liquids in GaAs/AlGaAs systems¹², this would yield for GaN/AlGaN an addition of $\mathcal{E}_4^x = 17 \text{ meV}$ (at 25 T) and $\mathcal{E}_6^x = 13 \text{ meV}$ (at 18 T) to the activation energy values. This is far beyond the experimental observation. On the other hand, in GaN based structures electrons have such a heavy mass that the Landau quantization energy $\hbar\omega_c$ over the whole regime of ‘intermediate’ magnetic fields studied is less than or, at least, comparable to the interaction energy, so the incompressibility argument [13] can no longer be applied as the reason for the use of the unscreened Coulomb potential in equation (5). This must be corrected by taking into account screening of the Coulomb interaction by Landau level mixing. In the following estimations, we make an extreme assumption that the Landau level mixing is so strong that the electron–electron interaction is screened as efficiently as in a perfect 2D metal. Then, we use such a screened potential for the estimate in equation (5). In a two-dimensional electron gas, screening takes

¹² Without screening, for a shallow electron gas buried at the distance $d \approx 200 \text{ \AA}$ from the surface of a semiconductor,

$$V(r) = \frac{e^2}{\chi} \left[\frac{1}{r} + \frac{(\chi - 1)/(\chi + 1)}{\sqrt{r^2 + 2(d/\lambda)^2}} \right].$$

place at distances comparable to the donor related Bohr radius, $a = \chi \hbar^2 / e^2 m^*$, and

$$V(r) = \frac{e^2}{\chi} \int_0^\infty \frac{J_0(qr)q \, dq}{q + a^{-1}} \approx \frac{e^2}{\chi r} \times \begin{cases} (a/r)^2, & r > a; \\ 1, & r < a; \end{cases}$$

where J_0 is the Bessel function. For the case of intermediate fields, $a < \lambda$, perfect screening of the long range part of the bare e–e repulsion would lead to the disappearance of \mathcal{E}_{2n+2}^x , since the short range part of $V(r)$ is irrelevant in the integral in equation (5): the latter integral is dominated by the contribution from $x \sim 1$, that is, from distances $r = \lambda\sqrt{2x} > a$. On the other hand, screening is never complete in a two-dimensional gas [20], due to the finite quadrupole moment of the resulting charge distribution, which results in a residual long range tail $V(r) = \frac{e^2 a^2}{\chi r^3}$. Taking into account this tail is the way to expand the Coulomb correction to the activation energy with respect to a small parameter $r_s^{-1} = \sqrt{a^2 n_e} \ll 1$. The contribution in the leading order in r_s^{-1} ,

$$\mathcal{E}_{\text{even}}^x \approx \kappa \hbar \omega_c \quad \text{with } \kappa = \frac{4\sqrt{2}}{3\sqrt{\pi}} \sqrt{a^2 n_e} \approx \frac{1.06}{r_s}, \quad (6)$$

was obtained after substituting $V(r) = \frac{e^2 a^2}{\chi r^3}$ into equation (5). Because at short distances ($r \sim a < \lambda$) the effect of the interaction in the integral in equation (5) is diminished, the use of such a divergent potential leads to only a slight overestimation of the result, which is of the order of $a^2 n_e$ and, therefore, appears in the next order of expansion in r_s^{-1} .

When deriving the result in equation (6), we used the ‘semiclassical’ asymptotes for the Laguerre polynomial functions with $n \gg 1$,

$$L_n(x) \rightarrow e^{x/2} J_0(\sqrt{2x(2n+1)}), \\ \frac{e^{-x}}{x} [L_n(x) - L_{n+1}(x)]^2 \rightarrow \frac{2}{2n+1} J_1^2(\sqrt{2x(2n+1)}),$$

so the result of the integration can be represented as

$$\mathcal{E}_{2n+2}^x \approx \frac{e^2 a^2}{\chi \lambda^3} \frac{2(n+1)}{\sqrt{2n+1}} \int_0^\infty dz \frac{J_1^2(z)}{z^2}, \quad (7)$$

where

$$\int_0^\infty dz \frac{J_1^2(z)}{z^2} = \frac{4}{3\pi}. \quad (8)$$

Then, we exploited the relationship between the Landau level index, filling factor and magnetic length, $2(n+1) = \nu = 2\pi\lambda^2 n_e$, and also the expression $\hbar\omega_c = \hbar^2/m^*\lambda^2$, to represent the resulting correction to the excitation energy for the electron gas with a fixed density n_e in equation (6) as a function of the z component of the magnetic field. For samples studied in the present work, $\chi = 8.9$; $n_e = (2.4\text{--}2.6) \times 10^{12} \text{ cm}^{-2}$, so $a^2 n_e \approx 0.16$. This yields $\kappa = 0.7 \pm 0.1$, comparable to the value $\kappa = 0.43 \pm 0.02$ obtained from the linear fit. The theoretical result (dashed–dotted line) is compared with experiment in figure 6. One can see that the calculations *done without any fitting parameter* give results that are close to the experimental observations. The theory slightly overestimates the observed cyclotron gap (effective mass) renormalization.

Finally, let us comment on the main experimental observation that can be deduced from figure 6: that the dependence of the \mathcal{E}_{2n+2} gap versus energy can be approximated as a linear one and its slope is different from that determined by the effective mass m^* and the g^* -factor. The gaps measured at 25 and 27 T are equal to 115 and 130 K and at 17 T are about 65 K. An overestimated error bar of these points is about ± 5 K, i.e., the size of points in the figure, while the error of the magnetic field is negligible. These four results alone allow one to establish

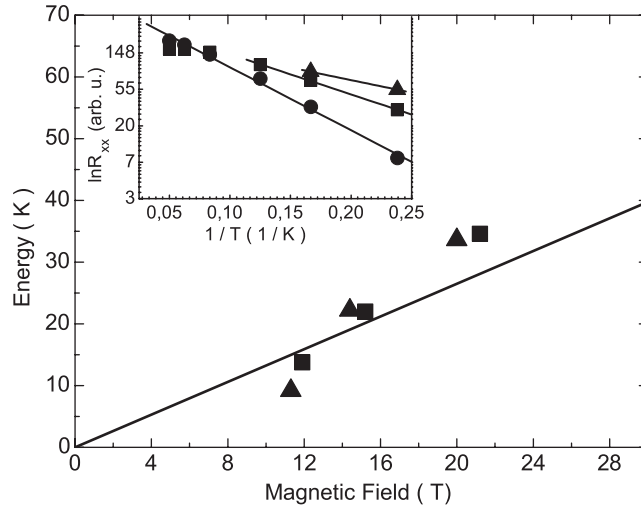


Figure 7. The magnetic field dependence of the R_{xx} activation energy for odd filling factors. Triangles and squares represent the data for two different carrier densities 2.4 and $2.6 \times 10^{12} \text{ cm}^{-2}$, respectively. The continuous line corresponds to the Zeeman splitting energy as determined by the tilted field experiments (linear coefficient 1.35 K T^{-1}). The inset shows the Arrhenius plots of R_{xx} data with linear fits for filling factors $\nu = 5$ (lowest line), 7 and 9 (highest line).

the slope of the solid line in figure 6. The results for lower magnetic fields follow the same linear dependence which shows that activation energy analysis can probably be also done for activation gaps that are below the Landau level width; taking them (or not) into account does not change the slope determined. The main final result is that the slope of the magnetic field dependence of \mathcal{E}_{2n+2} gaps is higher than that expected from a simple estimation based on the effective mass m^* and the g^* -factor. This ‘cyclotron gap enhancement’ may explain why the effective mass of the 2D electron determined in most SdHO transport activation measurements $0.18\text{--}0.20 m_e$ [21, 22] is smaller than that determined in cyclotron resonance experiments $0.23\text{--}0.25 m_e$ [4] (see footnote 11).

For completeness, the activation energy \mathcal{E}_{2n+1} is shown in figure 7. It is compared with the magnetic field dependence of the single-particle Zeeman energy $E_Z = g^* \mu B$ (solid line) calculated with the g -factor found in the tilted field experiment described in section 2. The energy gaps determined for odd filling factors \mathcal{E}_{2n+1} are relatively small—smaller than \mathcal{E}_{2n+2} and an estimated Landau level broadening (Γ 47 K). Uncertainties and error bars associated with the gaps deduced prevent a quantitative analysis of the gap versus B plots. Therefore, we cannot claim finding a difference between the observed \mathcal{E}_{2n+2} and \mathcal{E}_Z . The point is not only the precision or magnitude of the error bars but also the fact that the gaps experimentally obtained for \mathcal{E}_{2n+1} are smaller than the Landau level broadening (47 K). Please note however that a relatively strong disorder leading to the elastic Landau level broadening $\hbar/\tau_q \gg E_Z$ can suppress the net electron spin polarization and, therefore, diminish exchange effects at $\nu = 2n + 1$. Therefore the measured activation energies can be close to the single-particle energetic distance between two percolating states in the middle of spin-split Landau levels, $(n, +)$ and $(n, -)$.

Finally, we would like to point out that GaN/AlGaIn is a new 2DEG system. From the point of view of fundamental research, the 2DEG in a GaN/AlGaIn heterojunction is essentially different to the more standard 2DEG in a GaAs/GaAlAs heterostructure, because the electron mass and the bare g -factor in GaN are large. Experiments reported in this

work were performed on one of the highest quality samples (mobility $60\,000\text{ cm}^2\text{ V}^{-1}\text{ s}^{-1}$) and in very high permanent magnetic fields—up to 30 T. However, for more quantitative comparison of the theory with experiment, results in much higher magnetic fields and/or on higher mobility/quality samples are clearly needed, especially for odd filling factors.

4. Conclusions

A 2DEG with high mobility (above $60\,000\text{ cm}^2\text{ V}^{-1}\text{ s}^{-1}$ at 4 K) was obtained by MBE growth of dislocation free GaN and AlGaIn layers on bulk GaN substrates. Well resolved quantum Hall effect structures corresponding to cyclotron resonance and spin resonance splitting are observed. Results from two studies are reported:

- (i) a tilted field experiment determining the 2DEG g^* -factor from the angular modulation of the amplitude of SdH oscillations;
- (ii) quantum Hall effect measurements determining the activation energies for spin and cyclotron energy gaps at even and odd filling factors.

The observed ‘cyclotron gap’ enhancement is attributed to the effect of electron–electron interaction and is estimated using the model of a 2D-screened Coulomb potential. The analytic result for the enhancement of the ‘cyclotron gap’ yields an addition to the activation energy, $\mathcal{E}_{\text{even}}^x \approx \kappa \hbar \omega_c$ with $\kappa = 1.06/r_s$, and represents the first term in the expansion in the inverse of large r_s , $r_s^{-1} = \sqrt{a^2 n_e} \ll 1$. Both experimental and analytic results for the enhancement of the ‘cyclotron gap’ yield an addition to the activation energy, which is proportional to the magnetic field and therefore resembles the effective mass renormalization.

Acknowledgments

The authors thank R Haug, T Jungwirth, M Potemski, S Dmitriev, M Dyakonov and I Kukushkin for useful discussions. We acknowledge financial support from the EPSRC, EC High Field Infrastructure Network and NATO Collaborative Linkage Grant CLG-977520. Some of this work was done at the National High Magnetic Field Laboratory (USA), which is supported by NSF Cooperative Agreement No DMR-0084173 and by the State of Florida.

References

- [1] Gil B 1998 *Group III-Nitride Semiconductor Compounds: Physics and Applications* (Oxford: Clarendon) ISBN 0198501595
- [2] Pearson S 1999 GaN and related materials II *Optoelectronic Properties of Semiconductors and Superlattices* vol 7 (London: Gordon and Breach) pp 47–86
- [3] Asif Khan M *et al* 1992 *Appl. Phys. Lett.* **60** 3027
- [4] Knap W *et al* 1997 *Appl. Phys. Lett.* **70** 2123
Knap W *et al* 1996 *Solid State Commun.* **99** 195
- [5] Frayssinet E *et al* 2000 *Appl. Phys. Lett.* **77** 2551
- [6] Smorchkova I P *et al* 1999 *J. Appl. Phys.* **86** 4520
- [7] Manfra M J *et al* 2000 *Appl. Phys. Lett.* **77** 2888
- [8] Manfra M J *et al* 2002 *J. Appl. Phys.* **92** 338
- [9] Knap W *et al* 1999 *Appl. Phys. Lett.* **75** 3156
- [10] Brosig S *et al* 1998 *Physica B* **256–258** 239
Koch S *et al* 1993 *Phys. Rev. B* **47** 4048
- [11] Contreras S *et al* 2001 *J. Appl. Phys.* **89** 1251
- [12] Bychkov Y A and Rashba E I 1983 *Sov. Phys.—JETP* **58** 1062
- [13] Kallin C and Halperin B I 1984 *Phys. Rev. B* **30** 5655

-
- [14] Usher A *et al* 1990 *Phys. Rev. B* **41** 1129
Clark R G *et al* 1990 *Surf. Sci.* **229** 25
 - [15] Dunford R B *et al* 1998 *J. Appl. Phys.* **83** 3144
 - [16] Grandjean N *et al* 2000 *J. Appl. Phys.* **88** 183
 - [17] Tarasenko S A 2002 *Phys. Solid State* **9** 1769
 - [18] Du R R *et al* 1994 *Phys. Rev. Lett.* **73** 3274
 - [19] Lerner I V and Losovik Y 1980 *Sov. Phys.—JETP* **51** 588
 - [20] Ando T, Fowler A and Stern F 1982 *Rev. Mod. Phys.* **54** 437
 - [21] Elhamri S *et al* 1998 *Phys. Rev. B* **57** 1374
 - [22] Hang D R *et al* 2001 *Appl. Phys. Lett.* **79** 67